Received: 21 July 2022 | Revised: 4 January 2023 | Accepted: 6 January 2023

DOI: 10.1111/vru.13222

ORIGINAL INVESTIGATION

WILEY

CT features of divisional bile ducts in healthy Labrador Retrievers

Mirko Mattolini[1,2] | Simonetta Citi[2] | Beatrice Gianni[1] | Gregorio Carozzi[1] | Elvanessa Caleri[1] | Caterina Puccinelli[2] | Federica Rossi[1]

[1]Clinica Veterinaria dell'Orologio, Sasso Marconi, Bologna, Italy

[2]Department of Veterinary Sciences, University of Pisa, San Piero a Grado, Pisa, Italy

Correspondence
Mirko Mattolini, Clinica Veterinaria dell'Orologio, Sasso Marconi (BO), Italy, and Department of Veterinary Sciences, University of Pisa, San Piero a Grado (PI), Italy.
Email: mirko.mattolini@anicura.it

Abstract

Computed tomography (CT) is increasingly being used for the study of gallbladder and bile duct diseases. The first step in interpreting CT findings is understanding the cross-sectional anatomy of the structures involved, but there are no published studies describing the CT features of the divisional bile ducts. In dogs, anatomic studies report two common patterns including three or four divisional bile ducts. The aim of this retrospective, descriptive, anatomical study was to describe the size and pattern of the visible divisional bile ducts, based on their location and extension, using contrast-enhanced CT in a group of Labrador Retrievers without evidence of hepatobiliary diseases. The correlation between the biliary duct number and dimensions, and the visceral fat area percentage (VFA%) was also evaluated. The right lateral divisional duct (RLD) was visualized in four of 40 dogs, the left lateral divisional duct (LLD) in nine of 40 dogs, and in 17 of 40 dogs, both were simultaneously visualized. In 10 of 40 dogs, the RLD and LLD were not highlighted. When visible, the RLD has a median diameter of 0.23 cm and a median length of 0.82 cm. The LLD has a median diameter of 0.23 cm and a median length of 2.72 cm. The median diameter of the common bile duct before and after the insertion of divisional bile ducts was 0.23 and 0.25 cm, respectively. No correlation with the VFA% was found. At least one of the divisional bile ducts could be visualized using contrast-enhanced CT in the majority of sampled dogs (75%) .

KEYWORDS
biliary tract, CBD, CT, dog

1 | INTRODUCTION

Biliary tract diseases are common in dogs and frequently associated with early nonspecific clinical signs such as vomiting, diarrhea, lethargy, polyuria, polydipsia, and inappetence.[1] Usually, the clinical presentations of these diseases are the result of alteration or obstruction of the normal passage of bile.[2] In veterinary medicine, ultrasound (US) is the most commonly used diagnostic imaging modality to evaluate biliary diseases.[3-5] However, especially in large dogs with a deep abdomen, the sonographic evaluation of the small biliary ducts can be challenging and impaired by their distance from the abdominal wall,[6] greater amount of intraperitoneal fat,[7] and by the presence of intraluminal gas or food remnants in the gastrointestinal tract.[6,7] Cross-sectional diagnostic imaging modalities such as CT and magnetic resonance (MR)

Abbreviations: BCS, body condition score; CBD, common bile duct; CD, central division; CECT, contrast-enhanced computed tomography; CT, computed tomography; GB, gall bladder; LCD, left central duct; LLD, left lateral duct; RCD, right central duct; RLD, right lateral duct; VFA, visceral fat area; VFA%, visceral fat area percentage.

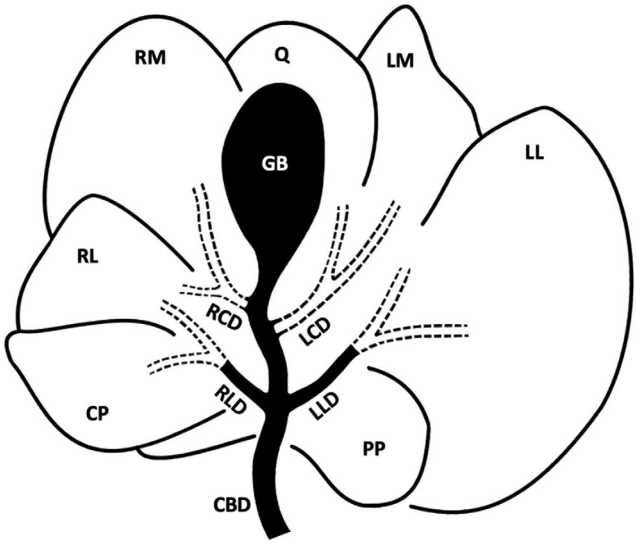

FIGURE 1 Schematic diagram of the four divisional bile ducts model and their relationship with the hepatic lobes. The dashed lines indicate the intraparenchymal non-visible portions of the divisional bile ducts, while the black structures are identified in CT. RCD, right central duct; LCD, left central duct; RLD, right lateral duct; LLD, left lateral duct; GB, gallbladder; CBD, common bile duct; CP, caudate process of the caudate lobe; RL, right lateral lobe; RM, right medial lobe; Q, quadrate lobe; LM, left medial lobe; LL, left lateral lobe; PP, papillary process of the caudate lobe

overcome these limitations, and some studies have been published with the aim of describing the normal anatomy and biliary pathology in small animals.[8-10] To improve the visualization of the intrahepatic biliary tract, several cholangiographic techniques have been proposed. Computed tomography cholangiography after intravenous (IV) administration of gadoxetic acid was successfully used in normal dogs[11] and attempted in healthy cats.[12] Meglumine iotroxate IV injection improved the evaluation in dogs with mucoceles in CT studies[13] and of cats with normal and obstructed biliary tract.[14] Magnetic resonance pancreatography after IV injection of secretin seems to be the best method to study the feline biliary tract by MR.[15] Finally, CT cholecystography after ultrasound-guided percutaneous contrast injection into the gallbladder (GB) allowed to depict the GB and the adjacent biliary tract in normal Beagles. The use of these techniques is limited by several reasons, including the failure in a percentage of cases, the lack of experience with diseased animals, the high cost of the contrast medium, and the time required to complete the study. The knowledge of the anatomy of the GB and bile ducts is crucial for imaging interpretation and during surgical cholecystectomy.[16]

Detailed anatomy of the common bile duct (CBD) and divisional bile ducts is reported in canine cadavers.[17,18] The CBD is formed after the last hepatic duct joins the excretory duct system, extends caudally to the duodenum, and ends at the major duodenal papilla 1.5 to 6.0 cm distal to the pylorus.[19] During this route, the CBD receives three or four hepatic ducts that drain the individual divisions of the liver.[17,18] When four divisional bile ducts are present, in particular 64%–70% of dogs[17,18] (Figure 1), two ducts drain the central division of the liver, one from the right medial lobe (right central duct, RCD) and one from the quadrate lobe (left central duct, LCD). These ducts enter the common bile duct immediately distal to the gallbladder; in most dogs (90%) the RCD is the most proximal followed by the LCD.[6] In the four-divisional duct model, the third duct drains the right hepatic division (right lateral lobe and caudate process of the caudate lobe—right lateral duct, RLD) and the fourth drains the left division (left lateral and left medial lobes—left lateral duct, LLD).[17,18] These last two ducts enter the CBD at the same level, in the mid-portion, with opposite orifices. In this model, the only reported anatomical variation is the end of the duct draining from the left medial lobe in the LCD rather than in the LLD.[17] The three divisional duct model (30%–36% of dogs[17,18]) has several anatomic variations. The most frequent is the drainage of the left medial lobe and left lateral lobe into the LCD rather than into the LLD.[18] In the second most common pattern, the left division of the liver drains via an auxiliary system located dorsally to the portal system (central division, CD) into the RCD.[17] The CD is a network of small bile ducts normally present in the bile duct system of dogs and many other animals. It connects the intrahepatic bile ducts of adjacent lobes and enables bile to drain when the primary ducts are obstructed.[17] Consequently, no lobe of the liver drains the bile independently from the others.[17] The papillary process of the caudate lobe is considered as a separate area of the liver since its drainage is variable and not closely associated with that of the rest of the right division of the liver.[17] As previously reported, a greater amount of intraabdominal adipose tissue may allow for better highlighting of some abdominal structures.[20] In fact, the fat surrounding a soft tissue structure makes it easier to differentiate from adjacent isodense structures.[20] In human medicine, CT is one of the most used methodologies for assessing visceral fat.[21] The visceral fat area (VFA) is defined as the fat area inside the abdominal musculature,[22,23] and is highly correlated with the visceral fat area percentage (VFA%). A previous CT study of the normal biliary system in dogs describes the CT features of the GB and of the CBD, however divisional bile ducts are not mentioned.[24] The limitations of the available cholangiographic techniques including low sensitivity, increased procedure time, and costs warrant further investigation of the standard examination.

For these reasons, the aim of this study was to describe the size and pattern of the divisional bile ducts in contrast-enhanced CT (CECT) sequences in a group of adult Labrador Retrievers without evidence of hepatobiliary diseases. The correlation between the number, length, and diameter of the visible ducts and the VFA% was also evaluated. We hypothesized that only the extrahepatic portion of the divisional ducts surrounded by visceral fat could be visualized and that there was a correlation between the number and the length of the visible divisional bile ducts and the VFA%.

2 | MATERIALS AND METHODS

2.1 | Selection and description of subjects

This study was a retrospective, descriptive, anatomical study. Approval by an institutional animal care and use committee or institutional review board was not required. Informed owner consent was obtained

in all the patients to perform the CT study. Medical records and CT studies of Labrador dogs presenting from October 2018 to March 2021 were collected from the database of the Clinica Veterinaria dell'Orologio in Sasso Marconi (Bologna, Italy).

Decisions regarding case selection were made by a European College of Veterinary Diagnostic Imaging (ECVDI)-certified veterinary radiologist (F.R.), and a first-year ECVDI resident (M.M.). Inclusion criteria for the study were a complete abdominal CECT study, and normal blood tests including hepatic profile. Patients presented with clinical and tomographic signs of hepatobiliary diseases, with large perihepatic masses or peritoneal effusion that prevented proper CT visualization of the area of interest between the visceral margin of the liver and the stomach were excluded.

2.2 | Data recording and analysis

The following data were recorded from the clinical database by a first-year ECVDI resident (M.M.): age at time of imaging, sex, weight at the time of imaging, and date of imaging.

All images were reviewed by the ECVDI-certified veterinary radiologist (F.R.), and a first-year ECVDI resident (M.M.). Images were analyzed and measurements were taken using an open-source dedicated DICOM viewer (Horos version 3.3.6, Horosproject.com). Window settings were adjusted as needed. The visible divisional bile ducts were classified based on their location, origin, and extension according to the previously mentioned classification (RCD, LCD, RLD, LLD). The laterality of divisional bile ducts was based on their origin from the right or left hepatic lobes and the entry point on the right or left aspect of CBD.

The following characteristics were recorded: presence, number, length, and diameter of each divisional bile duct. If no ducts were identified, this was also noted. The size of the visible CD network was also evaluated. Lastly, we measured the diameter of the CBD before and after the junction of the divisional bile ducts, when at least one of these was visible.

For all the included patients the VFA% was calculated as previously reported[22,23] by selecting a region of interest (ROI) based on the attenuation in the range of −135 to −105 Hounsfield units at the L3 slice level. Afterward, we considered only the area of adipose tissue inside the abdominal musculature, eliminating the subcutaneous fat, and dividing by the body area.

2.3 | Statistical analysis

All statistical analyses were selected and performed by a third-year Ph.D.-student veterinarian with course-work training in statistic (C.P.), using statistical analysis software (GraphPad Prism v. 9.0, GraphPad Software Inc, San Diego, CA, USA). The Shapiro–Wilk test was performed to assess the normality of data. Descriptive statistics were calculated. In addition, one-way ANOVA, followed by the Holm-Šídák multiple comparison test, and the Mann–Whitney test were used to evaluate the difference in VFA%, based on hepatic duct visualization. The Wilcoxon matched-pairs signed rank test was also used to assess the difference in diameter and length, between the different types of hepatic ducts both visualized in the same patients. Moreover, the Spearman rank correlation coefficient test was used to assess the correlation between the length of the visible portion of the divisional bile ducts and the VFA%. A P-value < 0.05 was considered statistically significant.

3 | RESULTS

3.1 | Study population

Forty Labrador Retrievers met the inclusion criteria. Median age at presentation was 9 years (range 2–13 years), and median body weight was 32.9 kg (range 15.5–52.5 kg). Of the total number, 16 (40%) were spayed females, five (12.5%) were neutered males, four (10%) intact females, and 15 (37.5%) intact males. Computed tomographies were performed in 30 dogs (75%) for staging neoplastic lesions at various sites, in three cases (7.5%) for lameness, in two dogs (5%) for investigation of non-neoplastic diseases, and one case each of pleural effusion, chronic cough, chronic otitis, spontaneous pneumothorax, and broncho-esophageal arteriovenous fistula, respectively.

3.2 | Imaging analysis

The CT studies were performed with a 16-slice CT unit (Bright Speed, GE Medical System, Bergamo, Italy). Dogs were examined under general anesthesia and placed in sternal recumbency. In all patients, expiratory apnea was induced always by hyperventilation and eventually with administration of a bolus of propofol immediately before the post-contrast scan. Images were acquired in helical scan mode, at 120 kV and 200—220 mA tube settings, a pitch of 0.562:1 and 1.25 mm slice thickness, with 50% overlap with a 0.7 s rotation time and reconstructed with a low-frequency algorithm (standard or detailed). Contrast-enhanced images were then obtained after intravenous injection of an iodinated contrast media (Ioversol, Optiray 300, Guerbet S.p.A, Milan) at a dosage of 640 mg I/kg, and with a 2–3 ml/s injection rate. The contrast media was followed by a saline flush with same injection rate via a dual-syringe injector system (OptiVantage®DH, Guerbet S.p.A, Milan). An injection-to-scan delay from the beginning of the injection of 30 s was used. If a multi-phase angio-CT was performed, the second (portal) scan phase acquired after 30 s post-injection was used.

Two divisional bile ducts (the RLD and LLD) were simultaneously visualized in 17 patients (42.5%), while in 13 of 40 (32.5%) dogs, only one hepatic divisional duct was visualized, the RLD in four of 40 patients (10%, Figure 2) and the LLD in nine of 40 dogs (22.5%), respectively. In 10 dogs, (25%) no ducts were highlighted. The two central divisional ducts (RCD and LCD) were not identified in any of the included patients.

In the transverse image, the visualized ducts appeared as round structures, located ventral to the portal vein, hypoattenuating to the hepatic parenchyma, and hyperattenuating to the peritoneal fat

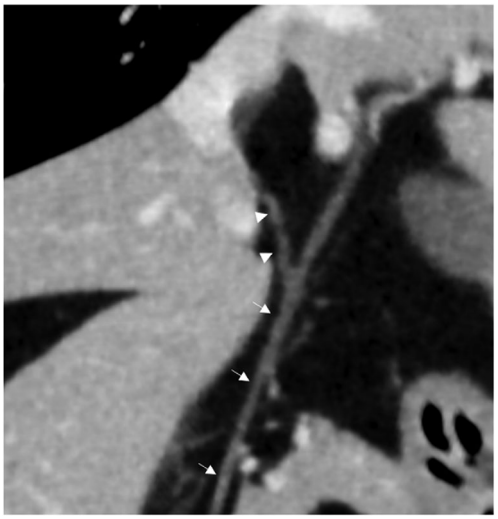

FIGURE 2 Multiplanar reconstruction of a dog where only the right lateral divisional bile duct (RLD—arrowheads) is visible that inserts into the common bile duct (CBD –slim arrows). CT image was reconstructed with a soft tissue algorithm, matrix 512 × 512, slide thickness 1.25 mm, 120 kV, 220 mA, pitch 0.562

FIGURE 3 Transverse view image of a dog where the right lateral divisional bile duct (RLD- arrowhead) and the left lateral divisional bile duct (LLD—thick arrow) are visualized just before insertion into the common bile duct (CBD—slim arrow). D, duodenum. CT image was reconstructed with a soft tissue algorithm, matrix 512 × 512, slide thickness 1.25 mm, 120 kV, 200 mA, pitch 0.562

(Figure 3). Multiplanar reconstructions permitted to recognize their path and relationship (Figures 4A and 4B).

The median length and diameter of the visualized RLDs and LLDs are reported in the Table 1. The CD network was not visualized in any patient. Table 2 summarizes the median CBD diameter before and after the insertion of the divisional biliary ducts. The mean percentage increase in the CBD diameter before and distally to the insertion of RLD and/or LLD was 15% (range 0–100%). The calculated VFA% had a median value of 7.73% (range 0.88%–17.21%).

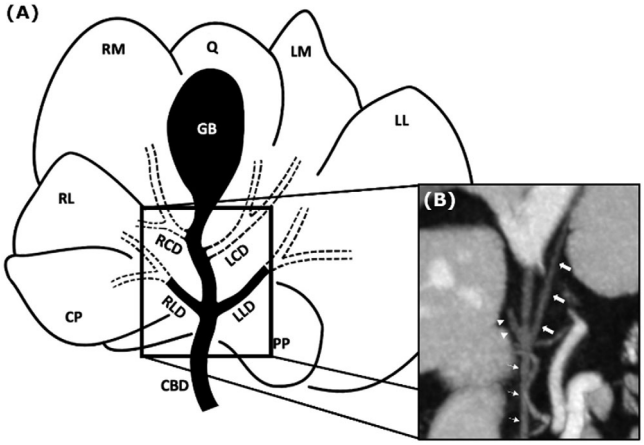

FIGURE 4 A, Schematic diagram of the four divisional bile ducts model focused on the visible portions of the divisional bile ducts. 4B, CT multiplanar reconstruction of a dog where the right lateral divisional bile duct (RLD—arrowheads) and the left lateral divisional bile duct (LLD—thick arrows) are visible. Note the insertion at the same level into the common bile duct (CBD—slim arrows). CT image was reconstructed with a soft tissue algorithm, matrix 512 × 512, slide thickness 1.25 mm, 120 kV, 220 mA, pitch 0.562. RCD, right central duct; LCD, left central duct; RLD, right lateral duct; LLD, left lateral duct; GB, gallbladder; CBD, common bile duct; CP, caudate process of the caudate lobe; RL, right lateral lobe; RM, right medial lobe; Q, quadrate lobe; LM, left medial lobe; LL, left lateral lobe; PP, papillary process of the caudate lobe

TABLE 1 Computed tomographic median length, median diameter, and range (under brackets) expressed in cm, of the right lateral divisional bile ducts (RLDs) and left lateral divisional bile ducts (LLDs)

	Median length (cm)	Median diameter (cm)
Total RLDs (n = 21)	0.82 (0.49–2.95)	0.23 (0.16–0.3)
Total LLDs (n = 26)	2.72 (1.42–3.97)	0.23 (0.13–0.33)
Simultaneously visualized RLDs + LLDs (n = 17)	0.82 (0.49–2.95) RLD[a] 2.71 (1.42–3.97) LLD[a]	0.23 (0.16–0.28) RLD[b] 0.23 (0.21–0.33) LLD[b]

Total RLDs and total LLDs = sum of all right and left measured ducts in 40 dogs. Simultaneously visualized RLDs + LLDs = measurements of the ducts in dogs where both right and left lateral divisional bile ducts were simultaneously visualized.

Abbreviations: LLD, left lateral divisional bile duct.; RLD, right lateral divisional bile duct.

[a]Median length of LLDs was significantly longer than the length of RLDs ($p < 0.0001$).

[b]Median diameter of LLDs was weakly significantly higher than the diameter of RLDs ($p = 0.02$).

3.3 | Statistical analysis

In the subgroup of patients where both RLD and LLD were visualized ($n = 17$), the length of LLDs was significantly longer than the length of RLDs ($P < 0.0001$, Figure 5); moreover, the diameter values were significantly different between RLDs and LLDs ($P = 0.02$, Figure 6). No

TABLE 2 Computed tomographic median diameter of the common bile duct before and after the insertion of the right lateral and/or left lateral divisional bile duct

	Median diameter before RLD and/or LLD insertion (cm)	Median diameter after RLD and/or LLD insertion (cm)
CBD	0.23 (0.15–0.36)	0.25 (0.16–0.45)

Abbreviations: CBD, common bile duct; LLD, left lateral divisional bile duct.; RLD, right lateral divisional bile duct.

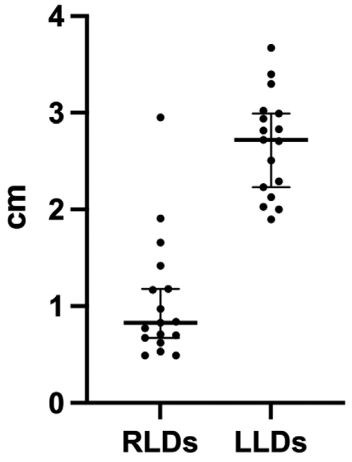

FIGURE 5 Scatter plot of RLDs and LLDs length values expressed in centimeters. RLDs, right lateral divisional bile ducts; LLDs, left lateral divisional bile ducts; cm centimeter

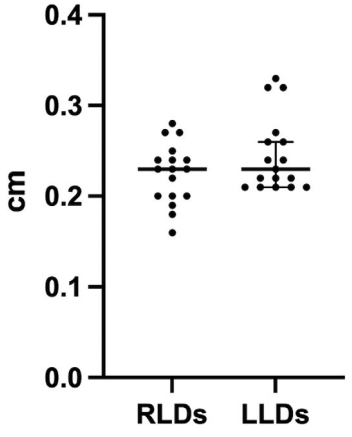

FIGURE 6 Scatter plot of RLDs and LLDs diameter values expressed in centimeters. RLDs, right lateral divisional bile ducts; LLDs, left lateral divisional bile ducts; cm, centimeter

statistical difference was found between the VFA% of dogs with no visualization of any duct, dogs with visualization of only one duct (RLD or LLD), and dogs with visualization of both RLD and LLD ($P = 0.22$). Moreover, no significant difference was found between the VFA% of dogs with no visualization of any duct and dogs with visualization of one or two ducts (RLD and/or LLD) ($P = 0.27$). In addition, the correlation between the length of the visible portion of the RLD or LLD and the VFA% was not statistically significant (P respectively of 0.8 and 0.33).

4 | DISCUSSION

The results of the current study supported our first hypothesis in that the extrahepatic portion of the lateral divisional bile ducts surrounded by visceral fat was visualized in a high percentage of dogs. In a population of normal Labrador Retrievers, at least one lateral divisional biliary duct was visualized in 75% of the animals. On the contrary, the second hypothesis of the study was not supported, since no statistically significant difference was found between the VFA% and divisional bile duct visualization.

In most of the patients (17 dogs, 42.5%), two opposite ducts were visualized, while in 13 of 40 patients (32.5%), only one of the lateral ducts was detected by CT. The mean length of the LLD was more than twice that of the RLD, and this difference was statistically significant ($P < 0.0001$). This probably reflects the normal anatomical position of these two divisional bile ducts. The CBD is a tubular structure that is formed after the last hepatic duct joins the excretory duct system, and it extends caudally and towards the right to the duodenum and ends at the major duodenal papilla. Consequently, being located to the left, the LLD has a longer path than the RLD to reach the CBD, and it is better visualized in CT. This might also explain why the LLD was identified more often than the RLD.

The median diameter of the LLD and RLD was similar, but when we evaluate the diameter values in the subgroup of patients where both RLD and LLD were visualized, the difference was weakly statistically significant ($P = 0.02$). In particular, the diameter values of LLDs seem to be higher than the RLDs, and this reflects the distribution of all data although the median is equal. This difference can be related to different sizes of the hepatic lobes drained by LLD (left lateral and left medial lobe) and RLD (right lateral lobe and caudate process of the caudate lobe).

The two central ducts (RCD and LCD) and the CD network were not identified in any of the included patients. The reasons for these features are the presence of isoattenuating liver parenchyma surrounding the small ducts and the short length of the ducts. In fact, RCD and LCD enter in the proximal part of the CBD, therefore their extrahepatic portion is very short.

The function of the CD network is to connect the intrahepatic bile ducts of adjacent lobes and to allow the drainage of the bile when the primary ducts are obstructed. Further studies in dogs with biliary ducts obstruction are needed to evaluate the visibility and size of the CD network in this clinical situation.

In 10 of 40 dogs (25%), no divisional bile ducts were visualized. This could be a consequence of the insufficient spatial resolution of CT with these small biliary structures, or in alternative real absence of the ducts because of anatomical variation.

In this study, the mean diameter of the CBD was 0.23 cm (range 0.15–0.36 cm) before the insertion of RLD and/or LLD and 0.26 cm (range 0.16–0.45 cm) distally. Our results are in accordance with the

CBD values previously reported in healthy dogs in CT.[25] Variations in the CBD diameter before and after the junction with RLD and LLD were not constant in our sample of dogs, ranging from 0% to doubling in size (100%). However, most of the dogs only showed a mild increase in diameter. Therefore, the increase in CBD diameter can be considered patient-dependent, depending on the biliary drainage or, possibly, on the patient's fasting.

The normal CBD is occasionally identified in US,[25] but especially in large, deep-chested dogs, or if the gastrointestinal tract content impairs the visualization of the porta hepatis, US can fail to identify this small structure and CT could be indicated. Moreover, biliary obstructive diseases are frequent in dogs and usually investigated with US. Previous studies have mainly focused on CBD obstructive diseases,[19,26] however there is increased interest in other biliary system abnormalities, for example, ductal plate malformation.[27-29]

Computed tomography is the most useful first-line imaging tool for the surgical planning in patients with biliary tract cancer or hepatic neoplasia in human medicine.[30] Cystic duct or common hepatic duct invasion are factors that predict a positive resection margin in these patients,[31] therefore a correct knowledge of the tomographic anatomy of these small biliary structures is mandatory.

Similarly, the involvement of divisional bile ducts or other biliary structures is important in dogs to evaluate the extent of liver masses for surgical planning and to minimize perioperative complications associated with hepatobiliary surgery.[33] CT could provide additional information especially in cases of liver masses or other perihepatic lesions adjacent to the hilus, where a connection or involvement of the biliary tract is unclear based on US. A better knowledge of the normal biliary duct anatomy could help the interpretation of the CT findings in these cases. On the other hand, masses originating from the liver or from organs adjacent to the hilus could prevent the proper visualization of these small bile structures because of compression or border effacement. Further studies are needed to investigate this. In alternative, the previously mentioned cholangiographic techniques may be useful to better evaluate the biliary tract in these situations.

In human medicine, CT is the gold standard for measuring VFA,[22,34] and the evaluation of this parameter has been related to several metabolic[35,36] and neoplastic diseases.[37,38]

Visceral fat area percentage has been calculated by CT and correlated with the body condition score (BCS) in dogs.[22,23] In this study, a correlation between the VFA% and the number, length, and diameter of the visualized divisional bile ducts was not found. Then, total intra-abdominal adipose tissue does not appear to be correlated with an improved visualization of these ducts. A reason that might explain this is the presence of other variables that can affect the visualization of ducts, for example, intrabdominal fat distribution or breed-related conformation. Indeed, previous canine studies involved dogs of different breeds and smaller sizes compared to our Labrador population.[23,24]

The main limitation of the present study is that the CT findings were not confirmed by a gold-standard imaging technique (CT or MRI cholangiography), or by dissection of canine specimens. This is needed to confirm the correspondence of the observed biliary duct pattern with the models described in anatomy. In fact, the lack of visibility of one or both ducts, as previously mentioned, could be a secondary to the insufficient spatial resolution of CT with these small structures, or real absence of the divisional bile ducts because of anatomical variation. This study cannot answer this question. On the other hand, a very large number of healthy dogs would be necessary to have all anatomical variations represented, which decreases the feasibility of the study and increases ethical concerns. Another limit of this study is the inclusion of only one canine breed. This was to reduce the variations due to different abdominal conformations. A final limitation is that the inter- and intraobserver agreement was not evaluated.

In conclusion, based on our review of the literature this is the first study describing the characteristics of the normal CT anatomy of the visible canine divisional bile ducts. This provides the basis for the correct identification of these normal structures in CT and could be useful for further studies in patients with hepatobiliary diseases.

LIST OF AUTHOR CONTRIBUTIONS

Category 1

(a) Conception and Design: Mattolini, Rossi
(b) Acquisition of Data: Mattolini, Gianni, Carozzi, Caleri, Rossi
(c) Analysis and Interpretation of Data: Mattolini, Citi, Puccinelli, Rossi

Category 2

(a) Drafting the Article: Mattolini, Puccinelli, Rossi
(b) Revising Article for Intellectual Content: Mattolini, Citi, Gianni, Carozzi, Caleri, Puccinelli, Rossi

Category 3

(a) Final Approval of the completed Article: Mattolini, Citi, Gianni, Carozzi, Caleri, Puccinelli, Rossi.

Category 4

(a) Agreement to be accountable for all aspects of the work in ensuring that questions related to the accuracy or integrity of any part of the work are appropriately investigated and resolved: Mattolini, Citi, Gianni, Carozzi, Caleri, Puccinelli, Rossi.

CONFLICT OF INTEREST STATEMENT

The authors have declared no conflict of interest.

PREVIOUS PRESENTATION OR PUBLICATION DISCLOSURE

The preliminary results of the present study were presented at a national congress in Italy (74° SISVET congress) as a short presentation in 2021.

EQUATOR NETWORK DISCLOSURE

no EQUATOR network checklist was used.

ORCID

Mirko Mattolini https://orcid.org/0000-0002-0065-2952
Simonetta Citi https://orcid.org/0000-0001-8211-9248
Caterina Puccinelli https://orcid.org/0000-0002-5313-0621

REFERENCES

1. Ettinger S, Feldman E, Coté E. *Veterinary Internal Medicine: Diseases of the Dog and the Cat*. 8th ed. Elsevier; 2017.
2. Bonagura DJ, Twedt DC. *Kirk's Current Veterinary Therapy XV*. 15th ed. Elsevier; 2014.
3. Jaffey JA, Graham A, VanEerde E, et al. Gallbladder mucocele: variables associated with outcome and the utility of ultrasonography to identify gallbladder rupture in 219 dogs (2007–2016). *J Vet Intern Med*. 2018; 32(1):195-200. doi:10.1111/jvim14898
4. Choi J, Kim A, Keh S, et al. Comparison between ultrasonographic and clicnical findings in 43 dogs with gallbladder mucoceles. *Vet Radiol Ultrasound*. 2014; 55(2):202-207. doi:10.1111/vru.12120
5. Wilkinson AR, DeMonaco SM, Panciera DL, et al. Bile duct obstruction associated with pancreatitis in 46 dogs. *J Vet Intern Med*. 2020; 34(5):1794-1800. doi:10.1111/jvim.15879
6. Marolf AJ. Diagnostic imaging of the hepatobiliary system: an update. *Vet Clin North Am - Small Anim Pract*. 2017; 47(3):555-568. doi:10.1016/j.cvsm.2016.11.006
7. Fields EL, Robertson ID, Osborne JA, et al. Comparison of abdominal computed tomography and abdominal ultrasound in sedated dogs. *Vet Radiol Ultrasound*. 2012; 53(5):513-517. doi:10.1111/j.1740-8261.2012.01949.x
8. Brand EM, Lim CK, Heng HG, et al. Computed tomographic features of confirmed gallbladder pathology in 34 dogs. *Vet Radiol Ultrasound*. 2020; 61(6):667-679. doi:10.1111/vru.12909
9. Fuerst JA, Hostnik ET. CT attenuation values and mineral distribution can be used to differentiate dogs with and without gallbladder mucoceles. *Vet Radiol Ultrasound*. 2019; 60(6):689-695. doi:10.1111/vru.12806
10. Marolf AJ. Computed Tomography and MRI of the Hepatobiliary System and Pancreas. *Vet Clin North Am - Small Anim Pract*. 2016;46(3):481-497. doi:10.1016/j.cvsm.2015.12.006
11. Chau J, Podadera JM, Young AC, et al. Use of gadoxetic acid for computed tomographic cholangiography in healthy dogs. *Am J Vet Res*. 2017;78(7):828-839. doi:10.2460/ajvr.78.7.828
12. Pilton JL, Chau J, Foo TS, et al. Hepatic computed tomography and cholangiography by use of gadoxetic acid in healthy cats. *Am J Vet Res*. 2019; 80(4):385-395. doi:10.2460/ajvr.80.4.385
13. Hayakawa S, Sato K, Sakai M, et al. CT cholangiography in dogs with gallbladder mucocoele. *J Small Anim Pract*. 2018; 59(8):490-495. doi:10.1111/jsap.12832
14. Tanaka T, Akiyoshi H, Mie K, et al. Drip infusion cholangiography with CT in cats. *J Feline Med Surg*. 2018; 20(12):1173-1176. doi:10.1177/1098612X17738615
15. Marolf AJ, Stewart JA, Dunphy TR, et al. Hepatic and pancreaticobiliary MRI and mr cholangiopancreatography with and without secretin stimulation in normal cats. *Vet Radiol Ultrasound*. 2011; 52(4):415-421. doi:10.1111/j.1740-8261.2011.01811.x
16. Kim D, Park S, Kim C, et al. Ultrasound-guided transhepatic computed tomography cholecystography in beagle dogs. *J Vet Sci*. 2019; 20(4):1-11. doi:10.4142/jvs.2019.20.e37
17. Murphy SM, Rodríguez JD, McAnulty JF. Minimally invasive cholecystostomy in the dog: evaluation of placement techniques and use in extrahepatic biliary obstruction. *Vet Surg*. 2007; 36(7):675-683. doi:10.1111/j.1532-950X.2007.00320.x
18. Sleight DR, Thomford NR. Gross anatomy of the blood supply and biliary drainage of the canine liver. *Anat Rec*. 1970; 166(2):153-160. doi:10.1002/ar.1091660204
19. Imagawa T, Ueno T, Tsuka T, et al. Anatomical variations of the extrahepatic ducts in dogs: knowledge for surgical procedures. *J Vet Med Sci*. 2010; 72(3):339-341. doi:10.1292/jvms.09-0196
20. Center SA. Diseases of the Gallbladder and Biliary Tree. *Vet Clin North Am - Small Anim Pract*. 2009; 39(3):543-598. doi:10.1016/j.cvsm.2009.01.004
21. Beukers M, Grosso FV, Voorhout G. Computed tomographic characteristics of presumed normal canine abdominal lymph nodes. *Vet Radiol Ultrasound*. 2013; 54(6):610-617. doi:10.1111/vru.12075
22. Wajchenberg BL. Subcutaneous and visceral adipose tissue: their relation to the metabolic syndrome. *Endocr Rev*. 2000; 21(6):697-738. doi:10.1210/edrv.21.6.0415
23. Ishioka K, Okumura M, Sagawa M, et al. Computed tomographic assessment of body fat in beagles. *Vet Radiol Ultrasound*. 2005; 46(1):49-53. doi:10.1111/j.1740-8261.2005.00009.x
24. Nagao I, Ohno K, Nagahara T, et al. Evaluation of visceral fat mass in dogs by computed tomography. *J Vet Med Sci*. 2019; 81(11):1552-1557. doi:10.1292/jvms.19-0254
25. Park HY, Cho YG, Lee YW, et al. Evaluation of gallbladder and common bile duct size and appearance by computed tomography in dogs. *J Vet Sci*. 2018; 19(5):653-659. doi:10.4142/JVS.2018.19.5.653
26. Mattoon JS, Sellon RK, Berry CR. *Small Animal Diagnostic Ultrasound*. 4th ed. Elsevier; 2021.
27. Gaillot HA, Penninck DG, Webster CRL, et al. Ultrasonographic features of extrahepatic biliary obstruction in 30 cats. *Vet Radiol Ultrasound*. 2007; 48(5):439-447. doi:10.1111/j.1740-8261.2007.00275.x
28. Pillai S, Center SA, McDonough SP, et al. Ductal plate malformation in the liver of boxer dogs: clinical and histological features. *Vet Pathol*. 2016; 53(3):602-613. doi:10.1177/0300985815610567
29. Sato K, Sakai M, Hayakawa S, et al. Gallbladder Agenesis in 17 Dogs: 2006–2016. *J Vet Intern Med*. 2018; 32(1):188-194. doi:10.1111/jvim.15034
30. Helgert ND, Sula MM. Caroli Syndrome in a 6-Year-Old Rottweiler Dog. *J Comp Pathol*. 2019; 167:1-5. doi:10.1016/j.jcps.2018.11.004
31. Choi SY, Kim JH, Lim S, et al. CT-based nomogram for predicting survival after R0 resection in patients with gallbladder cancer: a retrospective multicenter analysis. *Eur Radiol*. 2021; 31(5):3336-3346. doi:10.1007/s00330-020-07402-7
32. Choi SY, Kim JH, Park HJ, et al. Preoperative CT findings for prediction of resectability in patients with gallbladder cancer. *Eur Radiol*. 2019; 29(12):6458-6468. doi:10.1007/s00330-019-06323-4
33. Boothe HW. Current Concepts in Hepatobiliary Surgery. *Vet Clin North Am - Small Anim Pract*. 2015; 45(3):463-475. doi:10.1016/j.cvsm.2015.01.001
34. Furukawa K, Katabami T, Nakajima Y, et al. Evaluation of whole-abdominal fat volume by 700-slice CT scanning and comparison with the umbilical fat area anthropometric indices. *Obes Res Clin Pract*. 2010; 4(2):e111-e117. doi:10.1016/j.orcp.2009.10.001
35. Pickhardt PJ, Jee Y, O'Connor SD, et al. Visceral adiposity and hepatic steatosis at abdominal CT: association with the metabolic syndrome. *Am J Roentgenol*. 2012; 198(5):1100-1107. doi:10.2214/AJR.11.7361
36. Sato F, Maeda N, Yamada T, et al. Association of epicardial, visceral, and subcutaneous fat with cardiometabolic diseases. *Circ J*. 2018; 82(2):502-508. doi:10.1253/circj.CJ-17-0820
37. Goulart A, Malheiro N, Rios H, et al. Influence of visceral fat in the outcomes of colorectal cancer. *Dig Surg*. 2018; 36(1):33-40. doi:10.1159/000486143
38. Gao B, Liu Y, DIng C, et al. Comparison of visceral fat area measured by CT and bioelectrical impedance analysis in Chinese patients with gastric cancer: a cross-sectional study. *BMJ Open*. 2020; 10(7). doi:10.1136/bmjopen-2019-036335

How to cite this article: Mattolini M, Citi S, Gianni B, et al. CT features of divisional bile ducts in healthy Labrador Retrievers. *Vet Radiol Ultrasound*. 2023;64:448–454.
https://doi.org/10.1111/vru.13222